ORCA – Online Research @ Cardiff

This is an Open Access document downloaded from ORCA, Cardiff University's institutional repository:https://orca.cardiff.ac.uk/id/eprint/139795/

This is the author's version of a work that was submitted to / accepted for publication.

Citation for final published version:

Wang, Shuai, Shao, Longyi, Li, Jiaxu, Li, Jianan, Jones, Timothy , Zhu, Mingyu and Zhou, Jiamin 2021. Coal petrology of the Yimin Formation (Albian) in the Hailar Basin, NE China: paleoenvironments and wildfires during peat formation. Cretaceous Research , 104815. 10.1016/j.cretres.2021.104815

Publishers page: https://doi.org/10.1016/j.cretres.2021.104815

Please note:
Changes made as a result of publishing processes such as copy-editing, formatting and page numbers may not be reflected in this version. For the definitive version of this publication, please refer to the published source. You are advised to consult the publisher's version if you wish to cite this paper.

This version is being made available in accordance with publisher policies. See http://orca.cf.ac.uk/policies.html for usage policies. Copyright and moral rights for publications made available in ORCA are retained by the copyright holders.

Coal petrology of the Yimin Formation (Albian) in the Hailar Basin, NE China: paleoenvironments and wildfires during peat formation

Shuai Wang[a], Longyi Shao[a*], Jiaxu Li[a], Jianan Li[a], Timothy Jones[b], Mingyu Zhu[a], Jiamin Zhou[a]

a State Key Laboratory of Coal Resources and Safe Mining, College of Geoscience and Survey Engineering, China University of Mining and Technology (Beijing), Beijing 100083, China

b School of Earth and Environmental Sciences, Cardiff University, Park Place, Cardiff, UK

Corresponding author: Longyi Shao, College of Geoscience and Surveying Engineering, China University of Mining and Technology (Beijing), D11 Xueyuan Road, Haidian District, Beijing 100083, China. E-Mail: ShaoL@cumtb.edu.cn

Abstract: Coal seams preserve continuous and high-resolution records of paleoenvironments and wildfires events during peat accumulation. In order to elucidate wildfire characteristics and terrestrial climate changes during the time of peat accumulation, petrographic characteristics of coals in the Early Cretaceous Yimin Formation (Albian) in the Jiuqiao Sag, Hailar Basin, NE China were studied. Coal petrology analysis shows that the studied coal seams are characterized by dominant huminite (average 80.0 vol.%, mmf-mineral matter free), secondary inertinite (average 19.9 vol.%, mmf), and a very low mineral content (average 0.8 vol.%). These results suggest that the coal developed under waterlogged conditions in raised, ombrotrophic mires. The occurrence of moderate inertinite values in the coals implies that wildfires were frequent during the Albian. Burning temperature, ranging from 273 to 379 °C inferred from inertinite reflectances, indicates that wildfires during the Albian were ground fires because of low plant heights. Vertical trends in inertinite and huminite compositional changes within the coal seams may reflect local-scale, cyclic fluctuations in wildfire occurrence during the development of the peat mires. The likely cause of these fluctuations was changes in temperature and rainfall. The presence of significant levels of inertinite in the coals and inferred high atmospheric oxygen levels suggest that the Albian was a highly fire-prone period in the Hailar Basin. The recurrent occurrence of palaeo-wildfires events in the studied succession in the Hailar Basin reinforce that fire was an important element reaching wetland biodiversity during the Albian, while diversification and spread of angiosperms was taking place globally. Increased surface runoff and erosion after the palaeo-wildfires in the Jiuqiao Sag during the Albian may have enhanced the flux and availability of nutrients and siltation with sediment washing into fluvial, lacustrine and ocean systems, more or less contributing to the Albian anoxic events.

Key words： Albian; Hailar Basin; lignite; coal petrology; inertinite; wildfire

1 Introduction

Coal seams preserve abundant palaeoclimatic and palaeobotanic information and are sensitive to environmental changes through geological time (Teichmüller, 1989; Diessel, 1992). Within the Hailar Basin, coal seams have a relatively shallow burial depth (mostly < 1000 m), low coal rank (Ro, max < 0.5%), and anomalous thickness (up to 40 m) (Guo et al., 2018). The coal seams preserve continuous and *in-situ* records of peat accumulation (Wadsworth et al., 2010). Almost all inertinite (Fusinite, semifusinite and inertodetrinite) is believed to be the products of incomplete combustion as a result of wildfire (Scott, 2002; Glasspool and Scott, 2010). Some maceral formation in inertinite may be related to microbial and fungal oxidation after burial, such as macrinite, micrinite and funginite (Hower et al., 2013; O'Keefe et al., 2013). Vertical changes in inertinite and huminite in coals across the Cretaceous-Paleogene boundary have been used to infer cyclic fluctuations in wildfires (Jerrett et al., 2015).

Wildfires can impact on a large amount of biomass in many ecosystems, and can also play a significant role in biogeochemical cycles and in the selection and evolution of terrestrial biotas through geological time (Bowman et al., 2009; Belcher et al., 2010; He et al., 2012; Lamont and He, 2012; He et al., 2016; Lamont et al., 2019; He et al., 2019). Wildfire can be considered as a dominant ecological and evolutionary force promoting and maintaining biodiversity over numerous spatiotemporal scales through particular fire regimes (Bond and Keeley, 2005; He et al., 2019). In some ecological settings, the species composition, structure and plant traits are dominated by fire frequency and intensity (He et al., 2019). The spread of angiosperms in the Cretaceous was facilitated by low-intensity surface fires under high temperature, seasonally dry climates and higher than current atmospheric oxygen levels (Bond and Scott, 2010; Brown et al., 2012).

Fossil charcoal in sedimentary deposits has been widely used to study wildfires and their implications for palaeoclimates in deep time after the first appearance of terrestrial plants in the Silurian (Jones and Chaloner, 1991; Scott, 2002; Jasper et al., 2011; Petersen and Lindström, 2012; Tanner et al., 2012; Jasper et al., 2017; Sun et al., 2017; Wagner et al., 2017; El Atfy et al., 2019; Yan et al., 2019; Xu et al., 2020b). Experiments show that the minimum amount of oxygen needed to ignite and maintain a self-sustaining wildfire is between 13% (Jones and Chaloner, 1991) and 16% (Belcher et al., 2010). The abundance of charcoal in deposits is therefore partially controlled by the atmospheric oxygen content and this proxy can be used to reconstruct the atmospheric oxygen content over the past 450 million years (Glasspool and Scott, 2010; Shao et al., 2012; Glasspool et al., 2015). Polished charcoal surfaces under reflected light microscopy are used to infer the burning temperature and types of wildfire based on modern charring experiments (Jones et al., 1991; Guo and Bustin, 1998; Scott and Glasspool, 2005).

Cretaceous oceanic anoxic events have been widely recognised in the geological record by the occurrence of widespread black shales and carbon isotope excursions in organic-rich and carbonate rocks (Jenkyns, 2010; Jarvis et al., 2011; Baker et al., 2017; Xu et al., 2020a). An apparent increase of wildfire activity inferred by the rise in charcoal abundances (from 189 particles per g/TOM (total organic matter) to 5965 particles per g/TOM) at the initiation of Cretaceous anoxic events has been observed (Baker et al., 2020). Wildfire and associated post-fire erosion have a significant impact on the hydrological cycle through the burning of vegetation and litter layers and the erosion of soil after a rainfall event (Shakesby and Doerr, 2006; Moody et al., 2008; Muir et al., 2015). The removal of vegetation, litter and soil degradation can result in increased surface runoff and overland flow, promoting more nutrients being flushed into rivers, lakes and oceans, leading to elevated productivity and anoxic environments (Brown et al., 2012).

Although numerous studies have focused on the sedimentology, sequence stratigraphy and coal accumulation in the Early Cretaceous coal-bearing series of the Hailar Basin (Li, 1988; Zhang and Long, 1995; Guo et al., 2017; Li et al., 2018; Zhang et al., 2018b), few studies have dealt with the Early Cretaceous paleo-wildfires that occurred during peat formation in the Hailar Basin (Wang et al., 2019b). The paleo-fire events were inferred from the inertinite in the coals of the Early Cretaceous Yimin Formation and the atmospheric oxygen levels are suggested to be high at the time of peat accumulation (Wang et al., 2019b). Regionally, the Yimin Formation can be correlated with the Yingcheng Formation of the Songliao Basin by the *Ruffordia-Dryopterites* floral assemblages (Deng et al., 2012). The Yingcheng Formation contains volcanic and volcaniclastic rocks that have been assigned to 105–112 Ma by zircon U-Pb dating (Huang et al., 2011), therefore the Yingcheng

Formation and Yimin Formation can be attributed to the Albian. In order to better understand the role of wildfires on Cretaceous plant evolution and anoxic events, it is essential to identify the occurrences and characteristics of fossil charcoal (inertinite) and to interpret the mire settings in Cretaceous terrestrial deposits from the Hailar Basin, northeastern China. This study systematically documents the vertical changes in the petrological composition of mire deposits (coal seams) of the Jiuqiao Sag of the southeastern Hailar Basin, and interprets the paleoenvironments of these coal seams. This enables inferences to be made on the wildfire characteristics during times of peat accumulation and to interpret the possible relationships between wildfire and plant evolution, and anoxic events during the Albian.

2 Geological setting

The Hailar Basin is a large Mesozoic-Cenozoic continental fault-bounded basin developed on Hercynian folded basement (Guo et al., 2018; Liu et al., 2020a). It is situated on the western flank of the Great Xing'an Range and the southern Mongol-Okhotsk Suture (Han et al., 2018). The basin is characterized by a mainly northeast-trending structural grain, 4000–5000 M thickness of late Mesozoic–Cenozoic non-marine deposits and 16 sags that formed synchronously in an extensional tectonic regime (A et al., 2013). The basin can be divided into five tectonic units (Figure 1), from west to east consisting, respectively, of the Zalainuor Depression, Cuogang Uplift, Beirhu Depression, Bayanshan Uplift and Huhehu Depression (Guo et al., 2018). Lower Cretaceous coal-bearing strata comprise the Tongbomiao, Nantun, Damoguaihe, and Yimin formations from bottom to top (Figure 2), corresponding to early syn-rift, rift climax, late syn-rift and post-rift phases, respectively (Song et al., 2019). Sandy conglomerates, sandstones, siltstones, mudstones and lignites comprise the Lower Cretaceous strata (Guo et al., 2018). Palynology records from the Lower Cretaceous Yimin Formation in the Hailar Basin show that vegetation was mainly composed of coniferous forest and shrub, such as hygrophilous *Cyathidites* and *Pilosisporites*, indicating that a humid tropical climate prevailed (Zhang and Long, 1995; Wang et al., 2008).

This study focuses on the Jiuqiao Sag, which is located in the southeastern Hailar Basin, NE China (Figure 1). The Jiuqiao Sag is a graben with an area of approximately 2650 km^2, bounded by syn-depositional faults to the north-west and south-east (Zhang et al., 2018b). The Yimin Formation comprises conglomerates, sandstones, mudstones and lignites, which were deposited in fluvial-lacustrine environments (Zhang et al., 2018b). Thick-bedded conglomerates and sandy conglomerates with erosional surfaces, intercalated with thin-bedded siltstones and mudstones, are typical of braided fluvial depositional systems (Zhang and Long, 1995; Zhang et al., 2018b). Thick-bedded sandstones with planar and trough cross-beddings, interbedded with thick-bedded siltstones and mudstones, can be interpreted as fluvial delta depositional systems (Zhang and Long, 1995; Zhang et al., 2018b). Thick-bedded siltstones and mudstones with horizontal laminations, intercalated with fine-grained sandstones, typify lacustrine depositional systems (Zhang et al., 2018b). Coal seams A, B and C were developed in the braided delta plain depositional environment. The sediments underlying and overlying Seam A are siltstones. Seam B is underlain by siltstones and overlain by medium sandstones. The sediments underlying and overlying Seam C are fine sandstones (Figure 3).

Thick Albian coal seams are widely distributed in the Yimin Formation (Zhang and Long, 1995). The thicknesses of seams A, B and C are 12.8 m, 5.8 m and 0.6 m, respectively (Figure 3). Maximum huminite reflectance values of coal from the seams in the Jiuqiao Sag range from 0.34% to 0.43% with an average of 0.38% (Shao et al., 2020), indicating that the rank of coal seams A, B and C is lignite according to ASTM D388-05 (2005).

3 **Sample and analytical methods**

A total of 23 coal samples were collected from 3 coal seams at the H1 borehole (Figure 3). All samples were stored immediately in airtight plastic bags to protect them from contamination and oxidation. Sample number and location are shown in Figure 3. Maceral analyses were carried out on all the samples. Macroscopic charcoal fragments found in the coal samples were examined following the charcoal identification methods of Scott (2010). The small coal fragments were mounted on a stub and observed under Scanning Electron Microscopy (SEM).

Coal samples were crushed to less than 1 mm diameter and a portion of each sample was embedded in epoxy resin. After curing, the samples were polished according to standard methods (ISO 7404/2, 2009). Maceral classification and terminology in this study follow the conventional procedures (ICCP, 2001; Sýkorová et al., 2005) and the Chinese National Standard Method for Determining Maceral and Minerals in Coal (GB/T 8899-2013). Maceral analyses and inertinite reflectance measurements were carried out under white reflected and fluorescent light, with a 50x oil-immersion objective using a Leica DM4500P LED microscope (Leica, Wetzlar, Germany). For maceral analyses, a total of approximately 500 points in each polished block were counted (ISO 7404/3, 2009). For inertinite reflectance measurements, Yttrium Aluminum Garnet (YAG) (0.903%), Gadolinium Gallium Garnet (GGG) (1.719%), sapphire (0.590%) and optically black (zero) standards at 23 °C were employed, with a total of approximately 60 points counted in each polished block (ISO 7404/5, 2009). The testing results were converted into percentage values for each maceral and average inertinite reflectance values.

The temperature of wildfire combustion could be inferred from the measured inertinite reflectance values using the following equation: $T = 184.10 + 117.76 \times \%Ro$ (coefficient of determination $r^2 = 0.91$), where T is the burning temperature and %Ro is the measured inertinite reflectance (Jones 1997).

4 Results

The coal seams are well banded and are composed of bright, semi-bright, semi-dull, and dull coal lithotypes. Macroscopic charcoal fragments in the coals are characterized by black colour, visible streaks and silky luster, and show anatomical preservation under a hand lens. They are brittle and fragile.

Table 1 shows the maceral (vol. %, mmf) and mineral (vol. %) contents of coal seams A, B and C. Huminite is the most abundant maceral (63.8 vol.% to 97.4 vol.%) with an average of 80.0 vol.%. The main huminite macerals are eu-ulminite (Figures 4A, 4B), textoulminite (Figure 4C), and gelinite (Figure 4D), with average contents of 13.8 vol.%, 13.3 vol.%, and 47.1 vol.%, respectively. Inertinite content varies between 2.6 vol.% to 36.2 vol.%, with an average of 19.9 vol.% and is dominated by semifusinite and fusinite (Figures 4E, 4F, 4G) with average content of 11.9 vol.% and 7.3 vol.%, respectively. Inertodetrinite (Figure 4H) is also be found in the coals. Semifusinite and fusinite have visible homogenized cell walls (Figure 5), showing the anatomical characteristic which is consistent with the identification of angiosperms (Oakley and Falcon-Lang, 2009; Scott, 2010). Liptinite content is less than 1.5 vol.% with an average of 0.1 vol.%. Mineral content ranges from 0 to 2.6 vol.%, and average 0.8 vol.%. Different sized fragments of charcoal are found in coals, including micro-charcoal (< 180 μm) (Figures 4G), meso-charcoal (180 μm–1 mm) (Figures 4E, 4F) and macro-charcoal (> 1 mm) (Scott, 2010).

The vertical profiles of huminite and inertinite in each coal seam studied (Figure 6) show an obvious inverse relationship between huminite and inertinite. By subdividing coal seams into depositional units that exhibit either increasing-up or decreasing-up trends in huminite and inertinite content, the vertical trends of these indices in the three coal seams could be determined. As a result of this analysis, seams A, B and C are subdivided into 2 (A1 and A2), 3 (B1, B2 and B3) and 3 (C1, C2 and C3) depositional units, respectively.

The measured inertinite reflectance of the studied coals are shown in Figure 7. The inertinite reflectance ranges from 0.76%Ro to 1.66%Ro with an average value of 1.18%Ro. Calculated burning temperatures of the wildfires are 273–379 ℃ with an average value of 322 ℃, indicating lower temperature smoldering fires rather than high-temperature infernos.

5 Discussion

5.1 Mire environments during the Albian

The huminite, inertinite and mineral components in coals have been commonly used as indicators of paleoenvironmental conditions in ancient mires (Diessel, 2007; Jerrett et al., 2011; Petersen and Ratanasthien, 2011; Wang et al., 2019a; Wang et al., 2020). Huminite, mainly derived from the humification of vascular plant material, implies anaerobic conditions and indicates rapid burial of plant material. Liptinite is derived from hydrogen-rich plant components such as spores, resins, waxes and cuticles. Inertinite consists of the same plant material as huminite and liptinite, but underwent charring prior to humification (Scott, 2002). Mineral matter, represented by ash yields, is transported into the mires mainly through fluvial or marine inundation. Coals with a low mineral content and thus low ash yields (typically < 10% by volume) are interpreted as the product of raised, ombrotrophic mires and coals with high mineral matter (typically > 10% by volume) are interpreted as the product of low-lying, rheotrophic mires (Jerrett et al., 2015).

High levels of huminite (79.3 vol.%) and very low mineral (0.8 vol.%) contents of all the studied coal seams (Table 1) indicate waterlogged conditions prevailed in the raised, ombrotrophic mires, which can also be inferred from low ash yields (8.3%–22.7%) (Shao et al., 2020). The dynamics of modern ombrotrophic peats suggest that climate, especially rainfall, has a significant effect on their development (Opluštil and Sýkorová, 2018), which may be analogous to the mires that formed these Early Cretaceous coals. In SE Asia, ombrotrophic mires are characterized by annual rainfall between 2800 and 4700 mm, with an average of approximately 3600 mm (Page et al., 2006), which means the ombrotrophic mires can be maintained under high rainfall conditions. Therefore, it can be inferred that the precursor mire of coal seams A, B and C in Hailar Basin developed under high annual rainfall conditions.

5.2 Wildfire in the Albian peatland

The presence of moderate inertinite levels (19.8% vol.%) in the coal seams of the Jiuqiao Sag provides evidence of regular wildfires during deposition of the mire. Inertinites are characterized by relatively high reflectance, little or no fluorescence, high carbon and low hydrogen contents, and strong aromatization (Teichmüller, 1989; Scott, 2002). Fusinite and semifusinite are frequently found in inertinites. Both fusinite and semifusinite, as major maceral types of inertinite, have visible plant cellular structure (Figure 5), implying an origin as charcoal from paleo-wildfires (Scott, 2002). Cycles recorded by the vertical variations in abundance of inertinite and huminite composition of coals in the Jiuqiao Sag of the Hailar Basin (Figure 6) may reflect local-scale cyclic fluctuations in wildfires during the development of the peat mires. The occurrence of wildfires is typically facilitated by increased temperature and limited rainfall, although lightning for ignition, wind and sufficient fuel are also required (McKenzie et al., 2004; Daniau et al., 2012). For example, the regional-scale cyclic nature of inertinite and vitrinite distribution within the Cretaceous-Paleogene coals in western Canada suggests regional-scale cyclic changes in temperature and rainfall (Jerrett et al., 2015). The local and cyclic fluctuations in wildfires during the Albian are likely caused by cyclic fluctuations in temperature and rainfall.

Reconstructions of paleo-atmospheric oxygen levels based on diverse proxies demonstrated that, during the Albian, the atmospheric oxygen content was globally high (Bergman, 2004; Glasspool and Scott, 2010; Wang et al., 2019b). Atmospheric oxygen levels during the Albian could have been up to 29% (Glasspool and Scott, 2010), contributing to regular occurrence and distribution of wildfires in terrestrial ecosystems. With high atmospheric oxygen levels, wet vegetation could be more easily burnt, which could result in a higher frequency of fire events than in the present day. The records of inertinite in coals of the Jiuqiao Sag and inferred high atmospheric oxygen content are consistent with the assumption that the Albian was a high-fire period.

5.3 Wildfire and angiosperm evolution

The fossil record show that angiosperms were increasingly important plants during the Cretaceous and became dominant in the Late Cretaceous (Brown et al., 2012; Tao et al., 2013). Early flowering angiosperms were characterized by understory herbs and shrubs with little woody tissue until at least the Albian (Bond and Scott, 2010; Zhang et al., 2018a). Angiosperms had much higher maximum leaf vein densities and maximum photosynthetic rate than ferns and gymnosperms during the Cretaceous (Brodribb and Feild, 2010). Angiosperms had typically faster life cycles than gymnosperms so that the angiosperms could make fuller use of the essential nutrients released by wildfires (Zhang et al., 2018a). Rapid accumulation of biomass from angiosperms with high rates of primary productivity during the Early Cretaceous (Brown et al., 2012; Zhang et al., 2018a) would provide ample fuel for the occurrence and high frequency of wildfires under high atmospheric oxygen concentrations (He and Lamont, 2018), further facilitating the spread of angiosperms. Therefore, frequent fires would have increased the mortality rates and reduced the re-growth rates of trees. Therefore frequent wildfire could open up these enclosed forests, which provided more open sunlit environments for the expansion of the early angiosperms (Bond and Scott, 2010). Angiosperms are also capable of rapidly growing and surviving in disturbed environments, such as active stream systems or wet to aquatic environments (Feild et al., 2004; Brown et al., 2012).

All inertinites in Albian coals from the Jiuqiao Sag of Hailar Basin have a low inertinite reflectance (0.76%–1.66%) and low charcoal-forming burning temperature (273–379 ℃) indicating that they were derived from ground fires (Scott, 1989) and favouring the fast recovery of low-stature plants after a burn. Low-intensity ground fires do not typically kill the roots of plants. The weedy angiosperms were well adapted to ground fire, being able to resprout quickly from their roots (Brown et al., 2012). The charred angiosperms (Figure 5) in the Hailar Basin indicate early angiosperms provided fuels for the occurrence of wildfires. The evidence is consistent with angiosperms taking advantage of regular fire regimes resulting in their spread and diversification (Bond and Scott, 2010). Therefore, the recurrent occurrence of palaeo-wildfire events in the Hailar Basin strengthen that fire was an important element reaching wetland biodiversity during the Albian, while diversification and spread of angiosperms was taking place globally.

5.4 Wildfire and anoxic events

When fires damage the soil structure and vegetation cover, this promotes surface water runoff and erosion leading to increased transport and deposition (Shakesby and Doerr, 2006; Shakesby, 2011; Brown et al., 2012). Post-fire erosion can contribute to enhanced weathering production and the flux and availability of nutrients such as phosphorous from land to rivers, lakes and oceans (Kump, 1988; Lenton and Watson, 2000; Glasspool et al., 2015; Yan et al., 2019). This potentially promotes the rapid growth of plankton that in turn can lead to anoxic lacustrine and oceanic environments (Berrocoso et al., 2010; Kraal et al., 2010; Brown et al., 2012; Liu et al., 2020b). Fire can also supplement the supply of phosphorous through aerosol inputs in the atmosphere as smoke, resulting in phosphorous open ocean deposition (Baker et al., 2020; Yan et al., 2019). Albian marine anoxic events coincided with high atmospheric oxygen levels (estimated about 25%) (Wang et al., 2019b) and the contemporaneous coals in the Hailar Basin contain moderate inertinite levels that suggest periods of frequent wildfire activity. Increased surface runoff and erosion after the palaeo-wildfires in the Jiuqiao Sag during the Albian may have played a key role in the flux and availability of nutrients, and the sedimentation in the related fluvial, lacustrine and marine systems, more or less resulting in the Albian marine anoxic events. Therefore, it is possible that Albian anoxic events are related to wildfires (Figure 8). Further study of fire records in black shales and contemporary coals are required to establish the importance of fires during Cretaceous anoxic events.

6 Conclusions

(1) Coal petrology shows the coals of the Early Cretaceous Yimin Formation in the Jiuqiao Sag of the Hailar Basin are dominated by huminite, with inertinite and a low mineral content, indicating waterlogged conditions prevailed in raised, ombrotrophic paleo-mires. Vertical huminite and inertinite compositional changes within the coals in the Jiuqiao Sag may reflect local cyclic fluctuations in temperature and rainfall during the development of the peat mires.

(2) The record of inertinite in coals and inferred high atmospheric oxygen levels suggest that the Albian Hailar Basin was highly fire-prone. Burning temperatures ranged from 273 to 379 °C inferred from inertinite reflectance, suggesting that the wildfires during the Albian were low-temperature ground fires.

(3) The recurrent occurrences of palaeo-wildfire events in the studied succession in the Hailar Basin reinforce that fire was a significant element reaching wetland biodiversity during the Albian, while diversification and spread of angiosperms was taking place globally.

(4) The increasing of surface runoff and erosion after the palaeo-wildfires in the Jiuqiao Sag during the Albian may have influenced the flux and availability of nutrients, and the sedimentation as well, in the related fluvial, lacustrine and marine systems, more or less contributing to the Albian marine anoxic events.

Acknowledgments

This research was supported by the National Natural Science Foundation of China (42002128), the National Science and Technology Major Project (2016ZX0504100-003), the Yue Qi Scholar Project of China University of Mining and Technology (Beijing), and the Central University Fundamental Research Fund (2010YD09). We thank editor-in-chief Eduardo Koutsoukos and three anonymous reviewers for their constructive suggestions improving the manuscript.

Data Availability

All data generated or analyzed during this study are included in the manuscript.

References

A, M., Zhang, F., Yang, S., Chen, H., Batt, G.E., Sun, M., Meng, Q., Zhu, D., Cao, R., Li, J., 2013. Early Cretaceous provenance change in the southern Hailar Basin, northeastern China and its implication for basin evolution. Cretaceous Research 40, 21–42.

ASTM (American Society for Testing and Materials) D388-05, 2005. Standard Classification of Coals by Rank. ASTM International, West Conshohocken, PA. Available at: www.astm.org.

Baker, S.J., Hesselbo, S.P., Lenton, T.M., Duarte, L.V., Belcher, C.M., 2017. Charcoal evidence that rising atmospheric oxygen terminated Early Jurassic ocean anoxia. Nature Communications 8, 15018.

Baker, S.J., Belcher, C.M., Barclay, R.S., Hesselbo, S.P., Laurin, J., Sageman, B.B., 2020. CO_2-induced climate forcing on the fire record during the initiation of Cretaceous oceanic anoxic event 2. Geological Society America Bulletin 132, 321–333.

Belcher, C.M., Yearsley, J.M., Hadden, R.M., McElwain, J.C., Rein, G., 2010. Baseline intrinsic flammability of Earth's ecosystems estimated from paleoatmospheric oxygen over the past 350 million years. Proceedings of the National Academy of Sciences 107(52), 22448–22453.

Bergman, N.M., Lenton, T.M., Watson, A.J., 2004. COPSE: a new model of biogeochemical cycling over Phanerozoic time. American Journal of Science 304, 397–437.

Berrocoso, A.J., MacLeod, K.G., Martin, E.E., Bourbon, E., Londoño, C.I., 2010. Nutrient trap for Late Cretaceous organic-rich shales in the tropical North Atlantic. Geology 38, 1111–1114.

Bond, W.J., Keeley, J.E., 2005. Fire as global 'herbivore': the ecology and evolution of flammable ecosystems. Trends in Ecology and Evolution 20, 387–394.

Bond, W.J., Scott, A.C., 2010. Fire and the spread of flowering plants in the Cretaceous. New Phytologist 188(4), 1137–1150.

Bowman, D.M.J.S., Balch, J.K., Artaxo, P., et al., 2009. Fire in the Earth system. Science 324, 481–484.

Brodribb, T.J., Feild, T.S., 2010. Leaf hydraulic evolution led a surge in leaf photosynthetic capacity during early angiosperm diversification. Ecology Letters 13(2), 175–183.

Brown, S.A.E., Scott, A.C., Glasspool, I.J., Collinson, M.E. 2012. Cretaceous wildfires and their impact on the Earth system. Cretaceous Research 36(2): 162–190.

Daniau, A.-L., et al., 2012. Predictability of biomass burning in response to climate changes. Global Biogeochemical Cycles 26, GB4007.

Deng, S., Lu, Y., Fan, R., Li, X., Fang, L., Liu, L., 2012. Cretaceous floras and biostratigraphy of China. Journal of Stratigraphy 36(2), 241–265.

Diessel, C.F.K., 2007. Utility of coal petrology for sequence-stratigraphic analysis. International Journal of Coal Geology 70, 3–34.

El Atfy, H., Anan, T., Jasper, A., Uhl, D., 2019. Repeated occurrence of palaeo-wildfires during deposition of the Bahariya Formation (early Cenomanian) of Egypt. Journal of Palaeogeography 8, 28.

Feild, T.S., Arens, N.C., Doyle, J.A., Dawson, T.E., Donoghue, M.J., 2004. Dark and disturbed: A new image of early angiosperm ecology. Paleobiology 30(1), 82–107.

Guo, B., Shao, L., Hilton, J., Wang, S., Zhang, L., 2018. Sequence stratigraphic interpretation of peatland evolution in thick coal seams: Examples from Yimin Formation (Early Cretaceous), Hailaer Basin, China. International Journal of Coal Geology 196, 211–231.

Guo, B., Shao, L., Ma, S., Zhang, Q., 2017. Coal-accumulating and coal-forming patterns within sequence stratigraphy framework of Early Cretaceous in Hailar basin. Coal Geology & Exploration 2017, 45, 14–19. (in Chinese with English abstract)

Guo Y, Bustin, R.M., 1998. FTIR spectroscopy and reflectance of modern charcoals and fungal decayed woods: Implications for studies of inertinites in coals. International Journal of Coal Geology 37, 29–53.

Glasspool, I.J., Scott, A.C., 2010. Phanerozoic concentrations of atmospheric oxygen reconstructed from sedimentary charcoal. Nature Geoscience 3(9), 627–630.

Glasspool, I.J., Scott, A.C., Waltham, D., Pronina, N., Shao, L., 2015. The impact of fire on the Late Paleozoic Earth system. Frontiers in Plant Science 6. Article 756, 14 pp.

Han, Z., Sun, X., Zhu, D., Tian, J., Wang, P., Zhang, X., 2018. Characteristics and factors controlling reservoir space in the Cretaceous volcanic rocks of Hailar Basin, NE China. Marine and Petroleum Geology 91, 749–763.

He, T., Lamont, B.B., 2018. Baptism by fire: the pivotal role of ancient conflagrations in evolution of the Earth's flora. National Science Review 5, 237–254.

He, T., Lamont, B.B., Manning, J., 2016. A Cretaceous origin for fire adaptations in the Cape flora. Scientific Reports 6, 34880.

He, T., Lamont, B.B., Pausas, J.G., 2019. Fire as a key driver of Earth's biodiversity. Biological Reviews 94, 1983–2010.

He, T., Pausas, J.G., Belcher, C.M., Schwilk, D.W., Lamont, B.B., 2012. Fire-adapted traits of Pinusarose in the fiery Cretaceous. New Phytologist 194(3), 751–759.

Hower, J.C., O'Keefe, J.M., Wagner, N.J., Dai, S., Wang, X., Xue, W., 2013. An investigation of Wulantuga coal (Cretaceous, Inner Mongolia) macerals: paleopathology of faunal and fungal invasions into wood and the recognizable clues for their activity. International Journal of Coal Geology 114, 44–53.

Huang, Q., Wu H., Wan, X., He, H., Deng, C., 2011. New progress of intergrated chronostratigraphy of the Cretaceous in Songliao Basin. Journal of stratigraphy 35(3), 250–257. (in Chinese with English abstract)

ICCP, 2001. The new inertinite classification (ICCP System 1994). Fuel 80, 459–471.

ISO 7404/2, 2009. Methods for the petrographic analysis of coals: Part 2. Method of preparing coal samples.

ISO 7404/3, 2009. Methods for the petrographic analysis of coals: Part 3. Method of determining maceral group composition.

ISO 7404/5, 2009. Methods for the petrographic analysis of coals: Part 3. Method of determining microscopically the reflectance of vitrinite.

Jarvis, I., Lignum, J.S., Gröcke, D.R., Jenkyns, H.C., Pearce, M.A., 2011. Black shale deposition, atmospheric CO_2 drawdown, and cooling during the Cenomanian-Turonian oceanic anoxic event. Paleoceanography 26, PA3201.

Jasper, A., Agnihotri, D., Tewari, R., Spiekermann, R., Pires, E. F., Da Rosa, Á. A. S., Uhl, D., 2017. Fires in the mire: repeated fire events in Early Permian 'peat forming' vegetation of India. Geological Journal 52(6), 955–969.

Jasper, A., Uhl, D., Guerra-Sommer, M., Bernardes-de-Oliveira, M. E. C., Machado, N. T. G., 2011. Upper Paleozoic charcoal remains from South America: Multiple evidences of fire events in the coal bearing strata of the Paraná Basin, Brazil. Palaeogeography, Palaeoclimatology, Palaeoecology 306(3-4), 205–218.

Jenkyns, H.C., 2010. Geochemistry of oceanic anoxic events. Geochemistry Geophysics Geosystems 11, Q03004.

Jerrett, R.M., Flint, S.S., Davies, R.C., Hodgson, D.M., 2011. Sequence stratigraphic interpretation of a Pennsylvanian (Upper Carboniferous) coal from the central Appalachian Basin, USA. Sedimentology 58, 1180–1207.

Jerrett, R.M., Price, G.D., Grimes, S.T., Dawson, A.T., 2015. A paleoclimatic and paleoatmospheric record from peatlands accumulating during the Cretaceous-Paleogene boundary event, Western Interior Basin, Canada. Geological Society of America Bulletin 127(11-12), 1564–1582.

Jones, T.P., 1997. Fusain in Late Jurassic sediments from Witch Ground Graben, North Sea, U.K. Mededelingen Nederlands Instituut voor. Toegepaste Geowetenschappen TNO 58, 93–103.

Jones, T.P., Scott, A.C., Cope, M., 1991. Reflectance measurements and the temperature of formation of modern charcoals and implications for studies of fusain. Bulletin de la Société Géologique de

France 162 (2), 193–200.

Jones, T.P., W.G. Chaloner., 1991. Fossil charcoal, its recognition and palaeoatmospheric significance. Palaeogeography, Palaeoclimatology, Palaeoecology, 97 (1–2): 39–50.

Kraal, P., Slomp, C.P., Forster, A., Kuypers, M.M.M., 2010. Phosphorous cycling from the margin to abyssal depths in the proto-Atlantic during anoxic event 2. Palaeogeography, Palaeoclimatology, Palaeoecology 195, 42–54.

Kump, L., 1988. Terrestrial feedback in atmospheric oxygen regulation by fire and phosphorous. Nature 335, 152–154.

Lamont, B.B., He, T., 2012. Fire-adapted Gondwanan Angiosperm floras evolved in the Cretaceous. BMC Evolutionary Biology 12(1), 223.

Lamont, B.B., He, T., Yan, Z., 2019. Fire as a pre-emptive evolutionary trigger among seed plants. Perspectives in Plant Ecology, Evolution and Systematics 36, 13–23.

Lenton, T.M., Watson, A.J., 2000. Redfield revisited: 2. What regulates the oxygen content of the atmosphere? Global Biogeochemical Cycles 14, 249–268.

Li, S., 1988. Fault Basin Analysis and Coal Accumulation. Beijing: Geological Publishing House (in Chinese).

Li, Z., Wang, D., Lv, D., Li, Y., Liu, H., Wang, P., Liu, Y., Liu, J., Li, D., 2018. The geologic settings of Chinese coal deposits. International Geology Review 60, 548–578.

Liu, B., Yang, Y., Li, J., Chi, Y., Li, J., Fu, X., 2020a. Stress sensitivity of tight reservoirs and its effect on oil saturation: A case study of Lower Cretaceous tight clastic reservoirs in the Hailar Basin, Northeast China. Journal of Petroleum Science and Engineering 184, 106484.

Liu, X., Hu, X., Li, J., 2020b. Cretaceous oceanic anoxic and oxic events. Chinese Journal of Nature 42, 1–8. (in Chinese with English abstract)

McKenzie, D., Gedalof, Z., Peterson, D.L., Mote, P., 2004. Climatic Change, Wildfire, and Conservation. Conservation Biology18(4), 890–902.

Moody, J.A., Martin, D.A., Cannon, S.H., 2008. Post-wildfire erosion response in two geologic terrains in the western USA. Geomorphology 95, 103–118.

Muir, R.A., Bordy, E.M., Prevec, R., 2015. Lower Cretaceous deposit reveals first evidence of a post-wildfire debris flow in the Kirkwood Formation, Algoa Basin, Eastern Cape, South Africa. Cretaceous Research 56, 161–179.

Oakley, D., Falcon-Lang, H.J., 2009. Morphometric analysis of Cretaceous (Cenomanian) angiosperm woods from the Czech Republic. Review of Palaeobotany and Palynology 153, 375–385.

O’Keefe, J.M.K., Bechtel, A., Christanis, K., Dai, S., DiMichele, W.A., Eble, C.F., Esterle, J.S., Mastalerz, M., Raymond, A.L., Valentim, B.V., Wagner, N.J., Ward, C.R., Hower, J.C., 2013, On the fundamental difference between coal rank and coal type. International Journal of Coal Geology 118, 58–87.

Opluštil, S., Sýkorová, I., 2018. Early Pennsylvanian ombrotrophic mire of the Prokop Coal (Upper Silesian Basin); what does it say about climate? International Journal of Coal Geology 198, 116–143.

Page, S.E., Rieley, J.O., Wüst, R., 2006. Lowland tropical peatlands of Southeast Asia. In: Martini, I.P., Martinez Cortizas, A., Chesworth, W. (Eds.), Peatlands: Evolution and Records of Environmental and Climate Changes. Elsevier.

Petersen, H.I., Lindström, S., 2012. Synchronous wildfire activity rise and mire deforestation at the Triassic–Jurassic Boundary. PLoS ONE 7(10), e47236.

Petersen, H.I., Ratanasthien, B., 2011. Coal facies in a Cenozoic paralic lignite bed, Krabi Basin, southern Thailand: Changing peat-forming conditions related to relative sea-level controlled watertable variations. International Journal of Coal Geology 87, 2–12.

Scott, A.C., 1989. Observations on the nature and origin of fusain. International Journal of Coal Geology 12, 443–475.

Scott, A.C., 2002. Coal petrology and the origin of coal macerals: a way ahead? International Journal of Coal Geology 50, 119–134.

Scott, A.C., Glasspool, I.J., 2005. Charcoal reflectance as a proxy for the emplacement temperature of pyroclastic flow deposits. Geology 33(7), 589–592.

Scott, A.C., 2010. Charcoal recognition, taphonomy and uses in palaeoenvironmental analysis. Palaeogeography, Palaeoclimatology, Palaeoecology 291, 11–39.

Shakesby, R.A., Doerr, S.H., 2006. Wildfire as a hydrological and geomorphological agent. Earth-Science Reviews 74(3-4), 269–307.

Shakesby, R.A., 2011. Post-wildfire soil erosion in the Mediterranean: Review and future research directions. Earth-Science Reviews 105(3-4), 71–100.

Shao L., Li J., Wang S., Hou H., Li J., Zhu M., 2020. Pore structures and fractal characteristics of liquid nitrogen adsorption pores in lignite in the Hailar Basin. Natural Gas Industry 40(5), 15–25. (in Chinese with English abstract)

Shao, L., Wang, H., Yu, X., Lu, J., Zhang, M., 2012. Paleo-fires and atmospheric oxygen levels in the latest Permian: evidence from maceral compositions of coals in Eastern Yunnan, Southern China. Acta Geological Sinica (English Edition) 86(4), 949–962.

Sun, Y., Zhao, C., Püttmann, W., Kalkreuth, W., Qin, S, 2017. Evidence of widespread wildfires in a coal seam from the middle Permian of the North China Basin. Lithosphere 9(4), 595–608.

Song, J., Liu, Z., Wang, C., Gao, X., Liu, X., 2019. Multistage structural deformations of a superimposed basin system and its tectonic response to regional geological evolution: A case study from the Late Jurassic-Early Cretaceous Tanan depression, Hailar-Tamtsag basin. Marine and Petroleum Geology 110, 1–20.

Sýkorová, I., Pickel, W., Christanis, K., Wolf, M., Taylor, G.H., Flores, D., 2005. Classification of huminite—ICCP system 1994. International Journal of Coal Geology 62, 85–106.

Tao, M., Cui, Z., Chen, G., 2013. Mesozoic sporo-pollen assemblages and climate fluctuations in northeastern China. Acta Micropalaeontologica Sinica 30(3), 275–287. (in Chinese with English abstract)

Tanner, L.H., Wang, X., Morabito, A.C., 2012. Fossil charcoal from the Middle Jurassic of the Ordos Basin, China and its paleoatmospheric implications. Geoscience Frontiers 3(4), 493–502.

Teichmüller, M., 1989. The genesis of coal from the viewpoint of coal petrology. International Journal of Coal Geology 12, 1–87.

Wadsworth, J., Diessel, C., Boyd, R., 2010. The sequence stratigraphic significance of paralic coal and its use as an indicator of accommodation space in terrestrial sediments, in Ratcliffe, K.T., Zaitlin, B.A., eds., Application of Modern Stratigraphic Techniques: Theory and Case Histories. Society for Sedimentary Geology Special Publication 94, 201–219.

Wagner, M., Wachowiak, J., Kowalczyk, J., Natkaniec-Nowak, L., Heflik, W., Georges, C., 2017. Petrographic and mineralogical studies of fossil charcoal from Sierra de Bahoruco (Barahona Province, Dominican Republic). International Journal of Coal Geology 173, 142–149.

Wang, D., Li, Z., Liu, H., Lyu, D., Dong, G., 2019a. The genetic environmental transformation mechanism of coal and oil shale deposits in eastern China's continental fault basins and the developmental characteristics of the area's symbiotic assemblages—taking Huangxian Basin as an example. Petroleum Science 16, 469–491.

Wang, L., Sun, Y., Qiao, X., Xue, Y., Jin, Y., 2008. The Early Cretaceous palynologic palaeoclimate of Hailar Basin. Petroleum Geology & Oilfield development in Daqing 27(5), 38–42. (in Chinese with English abstract)

Wang, S., Shao, L., Wang, D., Hilton, J., Guo, B., Lu, J., 2020. Controls on accumulation of anomalously thick coals: Implications for sequence stratigraphic analysis. Sedimentology 67: 991–1013.

Wang, S., Shao, L., Yan, Z., Shi, M., Zhang, Y., 2019b. Characteristics of Early Cretaceous wildfires in peat-forming environment, NE China. Journal of Palaeogeography 103(7): 1653–1690.

Xu, X., Shao, L., Lan, B., Wang, S., Hilton, J., Qin, J., Hou, H., Zhao, J., 2020. Continental chemical weathering during the Early Cretaceous Oceanic Anoxic Event (OAE1b): a case study from the Fuxin fluvio-lacustrine basin, Liaoning Province, NE China. Journal of Palaeogeography.

Xu, Y., Uhl, D., Zhang, N., Zhao, C., Qin, S., Liang, H., Sun, Y., 2020. Evidence of widespread wildfires in coal seams from the Middle Jurassic of Northwest China and its impact on paleoclimate. Palaeogeography, Palaeoclimatology, Palaeoecology 109819.

Yan, Z., Shao, L., Glasspool, I. J., Wang, J., Wang, X., Wang, H., 2019. Frequent and intense fires in the final coals of the Paleozoic indicate elevated atmospheric oxygen levels at the onset of the End-Permian Mass Extinction Event. International Journal of Coal Geology 2019, 75–83.

Zhang, C., Long, Y., 1995. Sedimentary facies characteristics and oil-gas distribution in the Hailar Basin. Petroleum Industry Press, Beijing, 103 pp.

Zhang, M., Dai, S., Du, B., Ji, L., Hu, S., 2018a. Mid-Cretaceous Hothouse Climate and the Expansion of Early Angiosperms. Acta Geologica Sinica - English Edition 92(5), 2004–2025.

Zhang, Y., Shao, L., Sun, Q., Shi, M., Wang, S., Fan, J., Sun, B., 2018b. Sequence-paleogeography and coal accumulation features of Jiuqiao Sag Yimin Formation in Hailar Basin. Coal Science and Technology 2018 46, 177–187. (in Chinese with English abstract)

Figures and Tables captions

Figure 1 Map showing tectonic units of Hailar Basin (Zhang and Long, 1995).

Figure 2 Stratigraphic chart of the Hailar Basin (Zhang and Long, 1995).

Figure 3 Summary column showing sedimentary facies of the Early Cretaceous Yimin Formation in the Jiuqiao Sag of the Hailar Basin from the H1 borehole.

Figure 4 Photomicrographs of typical coal macerals in the studied coals in the Early Cretaceous Yimin Formation of the Jiuqiao Sag of the Hailar Basin. Tex, textoulminite; Eu, euulminite; Ge, gelinite; Fu, fusinite; Ma, macrinite; Id, inertodetrinite. Fusinite shows high reflectance and well-preserved cellular structure. All scale bars are 50 μm.

Figure 5 Scanning electron microscope micrographs of inertinite in the studied coals in the Early Cretaceous Yimin Formation of the Jiuqiao Sag of the Hailar Basin. All micrographs show cross section of angiosperm charcoal with structured and homogenized cell walls. (A) Overview of cross-section of angiosperm vessels, showing the roundish shapes of tracheids (sample 121). Scale bar 20 μm. (B) Cross-section showing less roundish shapes of tracheids (sample 121). Scale bar 20 μm. (C) Charcoalified angiosperm showing vessels and homogenized cell walls (sample 121). Scale bar 20 μm. (D) Cross-section showing deformed tracheids (sample 121). Scale bar 10 μm.

Figure 6 Coal petrological properties of the coal seams A, B and C from the Early Cretaceous Yimin

Formation in the Jiuqiao Sag of the Hailar Basin. Seams A, B and C are subdivided into 2 (A1 and A2), 3 (B1, B2 and B3) and 3 (C1, C2 and C3) depositional units, respectively, indicating cyclic fluctuations in wildfire during the development of the peat mires.

Figure 7 Measured inertinite reflectance values and calculated burning temperatures ($T = 184.10 + 117.76 \times \%Ro$) of wildfires in the Early Cretaceous Yimin Formation coals of the Jiuqiao Sag of the Hailar Basin. Low inertinite reflectance values and low burning temperatures are interpreted to suggest that wildfires were ground fires.

Figure 8 Schematic model showing possible relationships between wildfires and anoxic events

Table 1 Maceral and mineral contents of the coal seams from the Early Cretaceous Yimin Formation in the Jiuqiao Sag of the Hailar Basin.

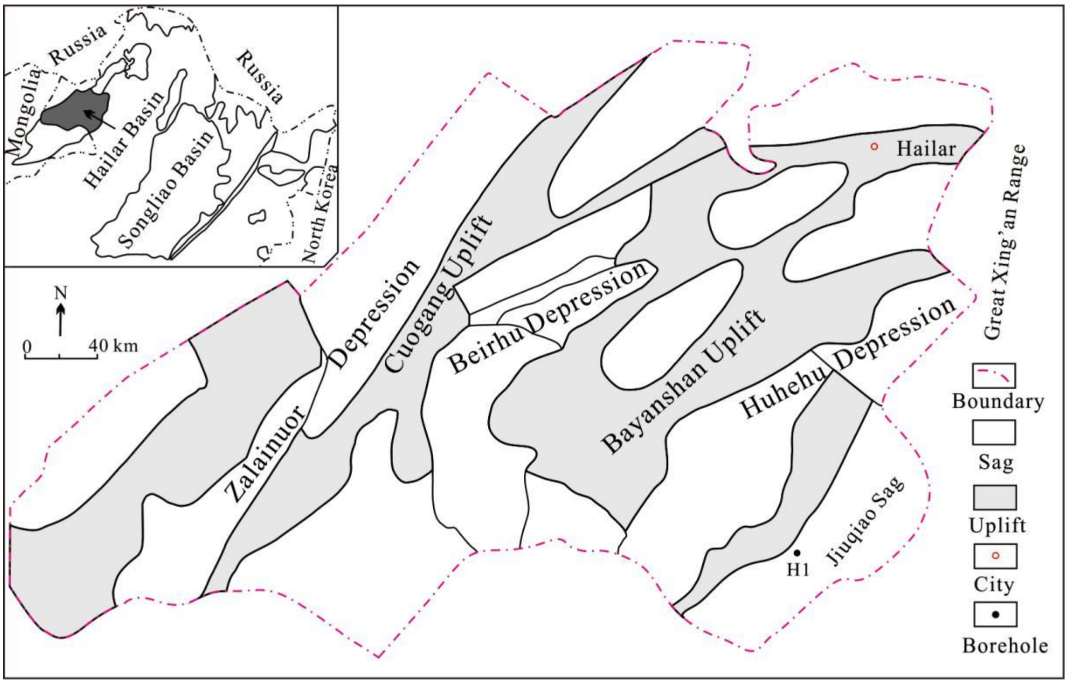

Figure 1 Map showing tectonic units of Hailar Basin (Zhang and Long, 1995).

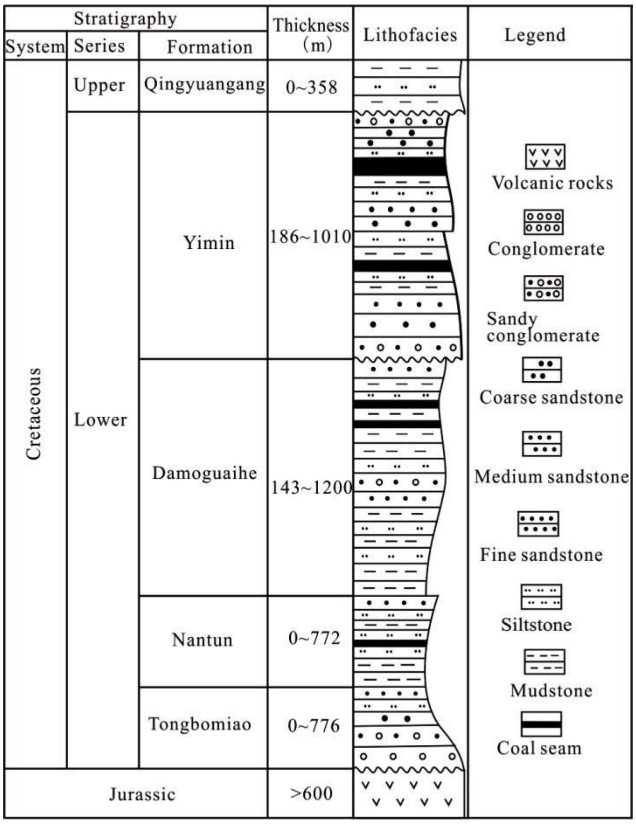

Figure 2 Stratigraphic chart of the Hailar Basin (Zhang and Long, 1995).

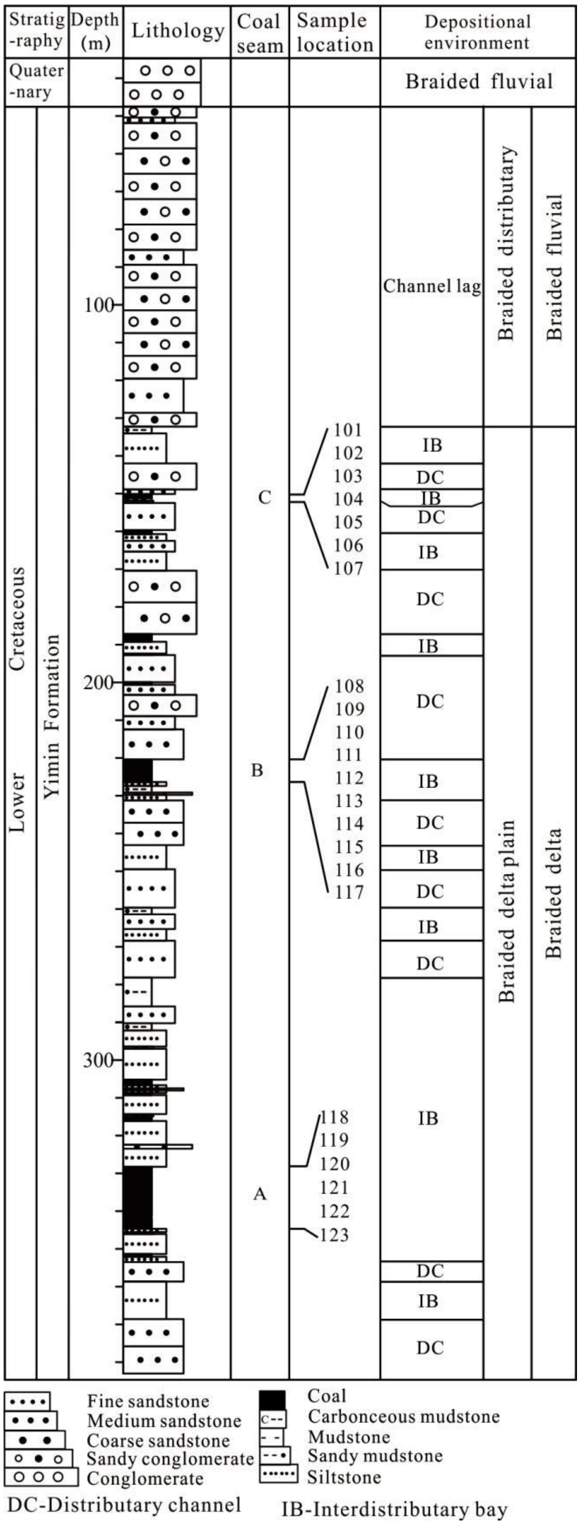

Figure 3 Summary column showing sedimentary facies of the Early Cretaceous Yimin Formation in the Jiuqiao Sag of the Hailar Basin from the H1 borehole.

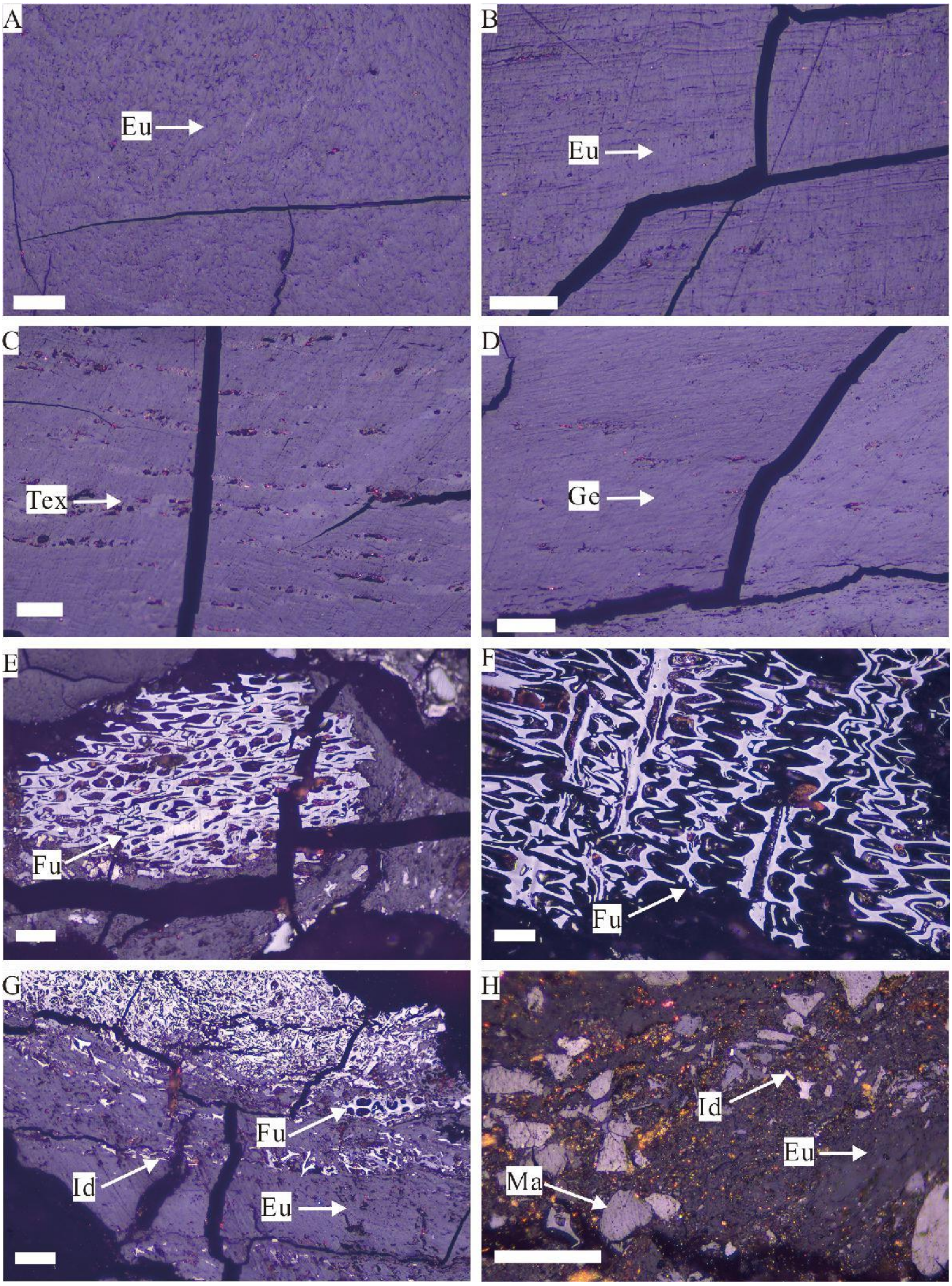

Figure 4 Photomicrographs of typical coal macerals in the studied coals in the Early Cretaceous Yimin Formation of the Jiuqiao Sag of the Hailar Basin. Tex, textoulminite; Eu, euulminite; Ge, gelinite; Fu, fusinite; Ma, macrinite; Id, inertodetrinite. Fusinite shows high reflectance and well-preserved cellular structure. All scale bars are 50 μm.

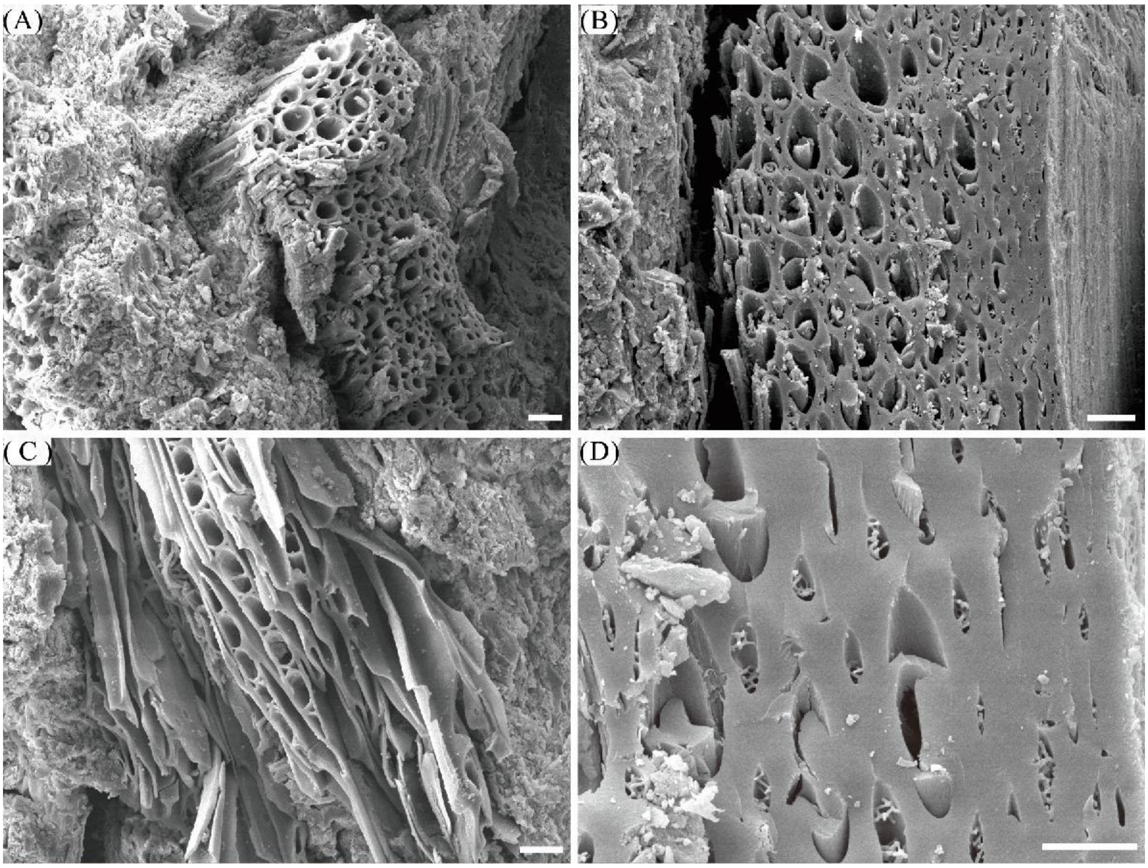

Figure 5 Scanning electron microscope micrographs of inertinite in the studied coals in the Early Cretaceous Yimin Formation of the Jiuqiao Sag of the Hailar Basin. All micrographs show cross section of angiosperm charcoal with structured and homogenized cell walls. (A) Overview of cross-section of angiosperm vessels, showing the roundish shapes of tracheids (sample 121). Scale bar 20 µm. (B) Cross-section showing less roundish shapes of tracheids (sample 121). Scale bar 20 µm. (C) Charcoalified angiosperm showing vessels and homogenized cell walls (sample 121). Scale bar 20 µm. (D) Cross-section showing deformed tracheids (sample 121). Scale bar 10 µm.

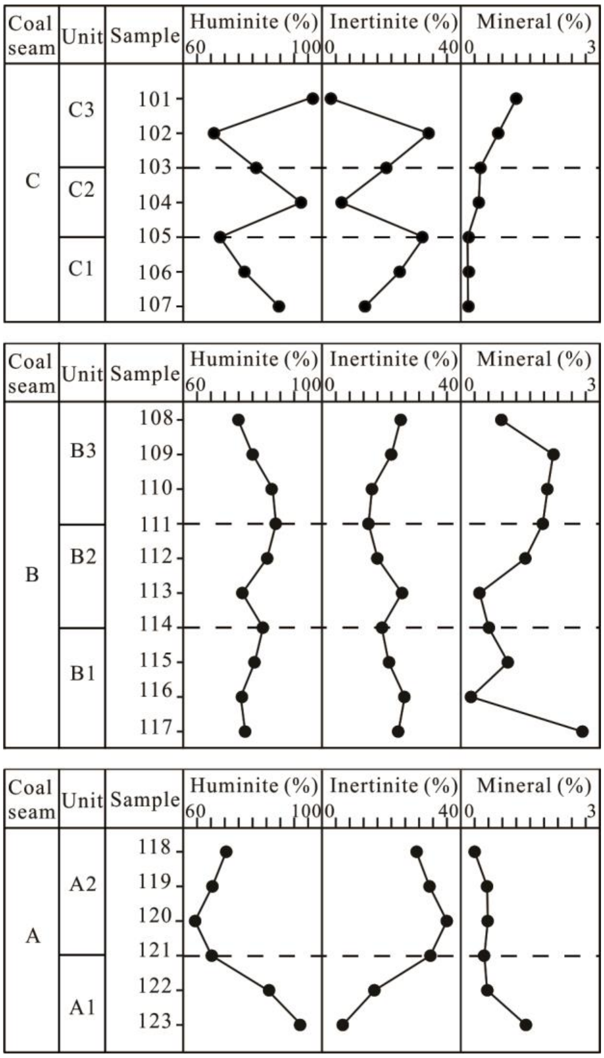

Figure 6 Coal petrological properties of the coal seams A, B and C from the Early Cretaceous Yimin Formation in the Jiuqiao Sag of the Hailar Basin. Seams A, B and C are subdivided into 2 (A1 and A2), 3 (B1, B2 and B3) and 3 (C1, C2 and C3) depositional units, respectively, indicating cyclic fluctuations in wildfire during the development of the peat mires.

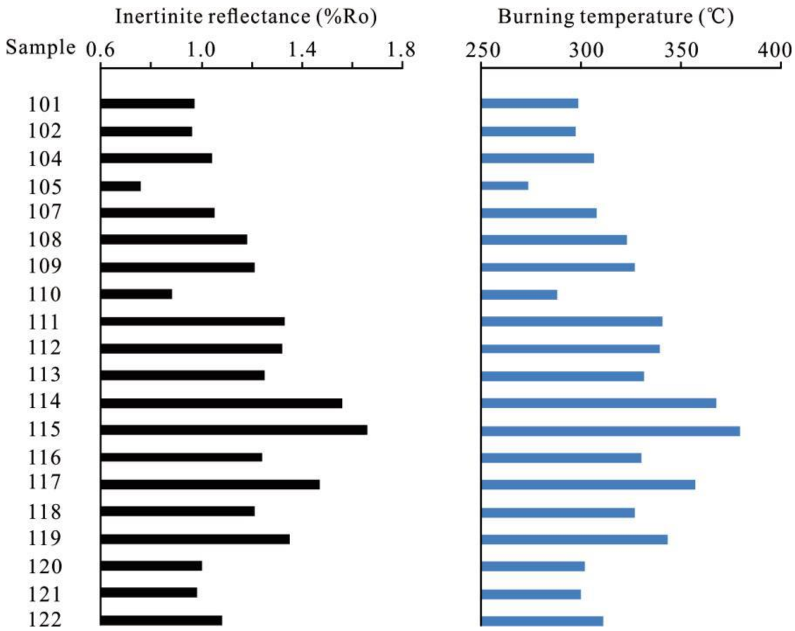

Figure 7 Measured inertinite reflectance values and calculated burning temperatures (T = 184.10 + 117.76 ×%Ro) of wildfires in the Early Cretaceous Yimin Formation coals of the Jiuqiao Sag of the Hailar Basin. Low inertinite reflectance values and low burning temperatures are interpreted to suggest that wildfires were ground fires.

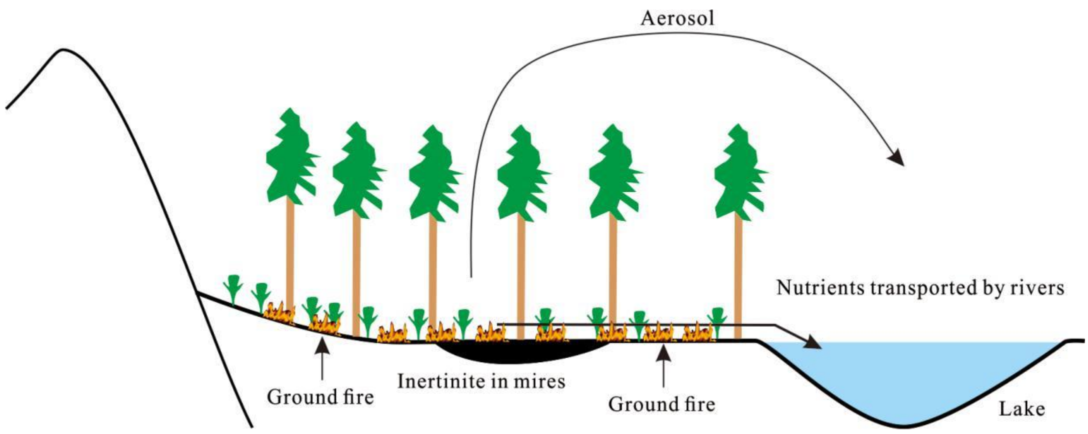

Figure 8 Schematic model showing possible relationships between wildfires and anoxic events

Table 1 Maceral and mineral contents of the coal seams from the Early Cretaceous Yimin Formation in the Jiuqiao Sag of the Hailar Basin.

Coal seam	Unit	Sample	Depth (m)	Huminite (vol.%, mmf)								Inertinite (vol.%, mmf)						Liptinite (vol.%, mmf)			Minerals (vol.%)			
				Te	Tex	Eu	At	De	Ge	Co	T-Hu	Fu	Sf	Fg	Ma	Id	T-In	Re	Su	T-Li	Cl	Ca	Qu	T-Mi
C	C3	101	150.6	2.3	10.6	27.4	1.2	0.0	55.6	0.3	97.4	1.7	0.5	0.0	0.2	0.2	2.6	0.0	0.0	0.0	0.9	0.3	0.0	1.2
		102	150.7	12.2	17.8	0.0	0.3	0.2	36.9	1.6	69.0	12.7	17.3	0.0	0.0	1.0	31.0	0.0	0.0	0.0	0.6	0.0	0.2	0.8
	C2	103	150.8	2.1	13.5	33.6	0.0	0.2	27.6	4.3	81.4	5.6	11.1	0.6	0.9	0.4	18.6	0.0	0.0	0.0	0.4	0.0	0.0	0.4
		104	150.9	2.9	37.2	0.0	0.4	0.0	52.8	1.0	94.3	3.1	2.3	0.0	0.0	0.2	5.7	0.0	0.0	0.0	0.2	0.0	0.2	0.4
	C1	105	151.0	4.2	13.2	8.1	0.0	0.0	45.1	0.0	70.6	11.7	17.7	0.0	0.0	0.0	29.4	0.0	0.0	0.0	0.0	0.0	0.0	0.0
		106	151.1	4.3	12.6	15.9	0.0	0.0	44.9	0.0	77.7	4.3	18.1	0.0	0.0	0.0	22.3	0.0	0.0	0.0	0.0	0.0	0.0	0.0
		107	151.2	3.8	18.5	1.0	0.3	0.8	63.3	0.0	87.6	2.8	6.1	0.0	0.0	3.5	12.4	0.0	0.0	0.0	0.0	0.0	0.0	0.0
B	B3	108	220.4	1.1	10.2	4.3	0.3	4.5	55.4	0.3	76.1	9.1	11.9	0.0	0.3	1.1	22.4	0.9	0.6	1.5	0.3	0.6	0.0	0.8
		109	221.0	6.8	23.7	0.8	0.2	1.0	46.5	1.0	80.1	9.5	9.3	0.0	0.0	1.2	19.9	0.0	0.0	0.0	1.0	0.8	0.2	2.0
		110	221.6	2.2	20.2	3.9	0.2	0.0	56.7	2.4	85.8	3.7	9.9	0.0	0.2	0.4	14.2	0.0	0.0	0.0	1.3	0.6	0.0	1.8
	B2	111	222.2	3.0	7.1	6.5	0.2	0.0	68.8	1.2	86.8	3.4	9.5	0.0	0.0	0.4	13.2	0.0	0.0	0.0	1.2	0.0	0.6	1.7
		112	222.8	1.4	9.0	13.3	0.0	0.2	59.8	0.7	84.3	5.9	8.6	0.0	0.5	0.7	15.7	0.0	0.0	0.0	0.9	0.3	0.2	1.4
		113	223.4	2.4	13.5	16.0	0.0	0.0	44.9	0.4	77.2	11.9	10.2	0.0	0.2	0.6	22.8	0.0	0.0	0.0	0.4	0.0	0.0	0.4
	B1	114	224.0	0.2	1.5	38.2	0.0	0.0	39.0	4.1	83.0	16.8	0.0	0.0	0.0	0.2	17.0	0.0	0.0	0.0	0.2	0.0	0.4	0.6
		115	224.6	2.2	12.3	16.7	0.0	0.0	49.1	0.6	80.9	7.6	11.3	0.0	0.0	0.2	19.1	0.0	0.0	0.0	0.6	0.2	0.2	1.0
		116	225.2	1.1	7.5	25.8	0.0	0.0	42.2	0.0	76.6	5.3	18.1	0.0	0.0	0.0	23.4	0.0	0.0	0.0	0.2	0.0	0.0	0.2
		117	225.8	2.3	6.1	23.0	0.2	0.0	45.0	1.3	77.9	8.4	13.3	0.0	0.2	0.2	22.1	0.0	0.0	0.0	1.7	0.7	0.2	2.6
A	A2	118	328.5	1.2	6.5	22.9	0.0	0.0	42.1	0.0	72.6	8.1	18.3	0.0	0.8	0.2	27.4	0.0	0.0	0.0	0.1	0.0	0.1	0.3
		119	330.5	12.2	9.9	6.5	0.0	0.0	39.0	1.3	68.8	12.2	17.9	0.0	0.6	0.6	31.2	0.0	0.0	0.0	0.6	0.0	0.0	0.6
		120	332.5	1.6	4.3	13.6	0.0	0.0	44.4	0.0	63.8	8.4	27.6	0.0	0.2	0.0	36.2	0.0	0.0	0.0	0.2	0.0	0.4	0.6

		121	334.5	20.3	17.4	0.3	0.0	0.0	28.4	2.2	68.6	10.8	19.4	0.0	1.0	0.2	31.4	0.0	0.0	0.0	0.5	0.0	0.0	0.5
	A1	122	336.5	8.5	11.9	16.0	0.0	0.0	48.5	0.0	84.8	2.5	12.7	0.0	0.0	0.0	15.2	0.0	0.0	0.0	0.2	0.0	0.4	8.5
		123	338.5	1.6	22.1	23.2	0.0	0.0	46.3	0.7	93.9	2.7	2.9	0.0	0.4	0.2	6.1	0.0	0.0	0.0	1.4	0.0	0.0	1.6

Te, textinite; Tex, textoulminite; Eu, euulminite; At, Attrinite; De, densinite; Ge, gelinite; Co, corpogelinite; T-Hu, total huminite; Su, suberinite; Re, resinite; T-Lp, total liptinite; Fu, fusinite; Sf, semifusinite; Fg, funginite; Ma, macrinite; Id, inertodetrinite; T-In, total inertinite; Cl, clay; Ca, Calcite; Qu, Quartz; T-Mi, total mineral; mmf-mineral matter free.